CHAPTER 177

Single-phase fluid modelling of sheet-flow toward the development of "numerical mobile bed"

by

Kazuo NADAOKA [1] and Hiroshi YAGI [2]

ABSTRACT

As a first step to develop "numerical mobile bed" as a promising tool for the study of sheet-flow problem, a computational scheme based on a single-phase fluid model has been constructed by formulating the vertical transport of mass and momentum within the sheet-flow layer. The numerical results have shown the satisfactory agreements with the experimental results in velocity profile, sediment transport rate, and others. Further the difference in the period of oscillation was found to have appreciable influence on the temporal evolution of the sheet-flow thickness, indicating the importance of unsteadiness in the sheet-flow dynamics.

1. Introduction

The sheet-flow is a mode of sediment transport in the condition of large bottom shear stress and has quite important role in nearshore sedimentary process because of its large transport rate. For the sheet-flow study, however, the efficiency of conventional approaches for sediment transport study, i.e., laboratory experiments and field measurements are limited because of the similitude problem for laboratory wave-flume experiments and the lack of measuring devices in field measurements. The use of U-shaped tank to generate oscillatory flow with large velocity amplitude is one of possible ways to avoid

1) Associate Professor, Department of Civil Engineering, Tokyo Institute of Technology, Tokyo 152, Japan.
2) Research Associate, Department of Civil Engineering, Tokyo Institute of Technology, Tokyo 152, Japan.

the similitude problem in the wave tank experiments (Horikawa et al. 1982, Sawamoto & Yamashita 1987). However, such simplification of the flow field from the original wave field into a pure sinusoidal oscillatory flow field may yield significant difference in the dynamics of the sediment movements in the sheet-flow layer, as demonstrated theoretically by Nadaoka et al. (1988, 1990).

As a promising tool to overcome these difficulties, the authors emphasize the need to develop the "numerical mobile bed (NMB)", corresponding to the recent idea of the "numerical wave tank" or "numerical wind tunnel". The benefits of NMB are quite obvious; i.e., it makes possible to simulate the sheet-flow under arbitrary wave conditions, and in the NMB we can easily see its internal structure.

Although two-phase fluid modelling is most desirable for the development of NMB, there exist no reliable constitutive equations to express the momentum transport through the sediment collision process, which is one of most essential processes in the sheet-flow dynamics. Hence in the present study, as a first step toward the development of NMB, a computational scheme based on a single-phase fluid concept has been constructed by modelling the vertical transport of mass and momentum within the sheet-flow layer.

2. Formulation and modelling of sheet-flow phenomenon

(1) Basic equations

For the "numerical wave tank" and "numerical wind tunnel", there exist definite basic equations, i.e., Laplace's equation and the Navier-Stokes equation, respectively. For the "numerical mobile bed (NMB)", however, the basic equation to describe the dynamical process of sediment-fluid mixture has not yet been well established in the form having universal applicability. This is mainly attributable to the fact that there exist no reliable ways to formulate the vertical transport of mass and momentum in the sheet-flow layer. Especially for the modelling of sheet-flow as two-phase fluid we have no constitutive equation to evaluate the momentum exchange through sediment collision described as follows, although the basic equations can be easily expressed in the two-phase forms as shown by, e.g., Kobayashi and Seo(1985).

Since the pioneering work by Bagnold(1954), many studies have been made for the additional shear stress attributable to the presence of solid particles, which is so-called "grain stress". According to Bagnold(1954), the flow regime of particle-laden two-phase flow can be divided into "grain-inertia region", "macro-viscous region", and "intermediate region" between them.

Estimates of order of magnitude can show that the sheet-flow in usual condition falls into the viscous or intermediate regions (e.g., Bakker and Kesteren, 1986). As the experimental formula of the grain stress, τ_g, for these regions, Bagnold(1954) suggested the following expression.

$$\tau_g = 2.25\lambda^{1.5}\mu_0\frac{\partial u}{\partial z} , \tag{1}$$

where λ is the linear concentration, μ_0 is the viscosity of intergranular fluid and $\partial u/\partial z$ is the rate of shearing. More recently Ahilan & Sleath (1987) arranged the experimental data by Savage and McKoewn (1983) and obtained the following formula of τ_g for the use in their numerical computation of oscillatory sheet-flow.

$$\tau_g = 1.2\lambda^2\mu_0\frac{\partial u}{\partial z} . \tag{2}$$

However, for the viscous region, the actual mixed shear stress cannot legitimately be split into grain and fluid elements as described by Bagnold(1954). This is reflected in the fact that these experimental formulae have the forms with linear dependence on the fluid viscosity μ_0; hence τ_g becomes zero as $\mu_0 \to 0$. Therefore these experimental formulae cannot be used for the expression of the shear stress due to the grain-grain interaction in the two-phase formulation.

Considering such state of the limited knowledge on the constitutive equations at present, we have adopted a single-phase fluid formulation as one of realistic approaches. In this formulation, the equations of motion can be express as

$$\frac{Du}{Dt} = -\frac{1}{\rho}\frac{\partial p}{\partial x} + \frac{1}{\rho}\left[\frac{\partial}{\partial x}\left(\mu_e\frac{\partial u}{\partial x}\right)+\frac{\partial}{\partial z}\left(\mu_e\frac{\partial u}{\partial z}\right)\right] + \frac{\partial}{\partial x}\left(\Omega_x\frac{\partial u}{\partial x}\right) + \frac{\partial}{\partial z}\left(\Omega_z\frac{\partial u}{\partial z}\right), \tag{3}$$

$$\frac{Dw}{Dt} = -\frac{1}{\rho}\frac{\partial p}{\partial z} + \frac{1}{\rho}\left[\frac{\partial}{\partial x}\left(\mu_e\frac{\partial w}{\partial x}\right)+\frac{\partial}{\partial z}\left(\mu_e\frac{\partial w}{\partial z}\right)\right] + \frac{\partial}{\partial x}\left(\Omega_x\frac{\partial w}{\partial x}\right) + \frac{\partial}{\partial z}\left(\Omega_z\frac{\partial w}{\partial z}\right), \tag{4}$$

where u and w are horizontal and vertical components of composite velocity of the sediment-fluid mixture, p is the pressure, ρ is the density of the mixture, Ω_x and Ω_z are x and z components of eddy viscosity, and μ_e is an equivalent viscosity to represent sediment collision effect. In order to obtain a closed system of the basic equations, we need further the continuity equation(5) and mass conservation equation(6) for the sediments.

$$\frac{\partial u}{\partial x} + \frac{\partial w}{\partial z} = 0, \tag{5}$$

$$\frac{\partial c}{\partial t} + \frac{\partial}{\partial x}(cu) + \frac{\partial}{\partial z}\{c(w-w_f)\} = \frac{\partial}{\partial x}\left(K_x\frac{\partial c}{\partial x}\right) + \frac{\partial}{\partial z}\left(K_z\frac{\partial c}{\partial z}\right), \tag{6}$$

in which c is the volumetric concentration of sediments, K_x and K_z are their horizontal and vertical diffusion coefficients, and w_f is the settling velocity of the sediment particles.

(2) Modelling of mass and momentum diffusivities and fall velocity of sediments

The accuracy of the present numerical model entirely depends on the way to specify the diffusion coefficients, μ_e, Ω_x, Ω_y, K_x, K_z and the settling velocity w_f. Unfortunately, however, there exist no established methods for the modelling of these quantities. Hence, in the present study, we have introduced tentative modellings of these factors as described in what follows.

a) Vertical diffusion coefficients of momentum

The factors governing the physical process of momentum exchange within the sheet-flow layer are

1) Momentum exchange through the sediment collision,
2) Viscous stress within the intergranular fluid,
3) Reynolds stress in the intergranular fluid.

Among these, in the present model, 1) and 2) are incorporated by an effective viscosity μ_e varying with sediment concentration c. The functional dependence of μ_e on c is assumed to be formulated as eq.(7) after Eilers (1941).

$$\frac{\mu_e}{\mu_0} = \left(1 + \frac{1.25c}{1-c/c_{max}}\right)^2. \tag{7}$$

In this formula, as c becomes the maximum possible concentration c_{max}, μ_e attains infinitely large value. This behavior of $\mu_e(c)$ near c_{max} is consistent with the fact that the particles with the concentration of c_{max} remain at rest. Although Eilers specified c_{max} to be 0.74, the concentration c for the real sand particles in the sheet-flow layer can attain 0.65 at most. Hence, in the present model, c_{max} is assumed to be 0.65. Furthermore, in order to avoid the infinitely large number to appear in the numerical calculation when c becomes c_{max}, eq.(7) has been slightly modified as eq.(8) for the use in the present numerical simulation.

$$\frac{\mu_e}{\mu_0} = \left[1 + \frac{1.25c}{1-0.95\left(c/c_{max}\right)}\right]^2. \tag{8}$$

Reynolds stress within the intergranular fluid is another important factor for momentum transfer in the sheet-flow layer and it may be formulated most simply through a mixing length theory such as

$$\Omega_z = l^2 \left|\frac{\partial u}{\partial z}\right|. \tag{9}$$

However, there arises a difficulty in the way to define the mixing length for the fluid domain with "fuzzy" boundary such as sheet-flow layer. Namely, for the sheet-flow with a typical vertical profile of the sediment concentration c as shown in Fig.1, the vertical location of the boundary can not be prescribed definitely. Hence, in the present study, a tentative new model of the mixing length has been introduced by considering a physical aspect of the eddy structure in the sheet-flow layer. Namely, within the sheet-flow layer, the eddy scale is not prescribed with the local concentration $c(z)$, but is considered to be governed by the overall feature of $c(z)$ profile. On the other hand, far above the sheet-flow layer, the layer acts as if it is a fixed boundary for the eddy structure. Hence at the far field above the sheet-flow layer, the mixing length should be almost coincide with that for the rigid boundary.

As one of possible models being consistent with these consideration, a new mixing model defined by equation (10) have been introduced, which is shown schematically by the solid curve for the mixing length $l(z)$ in Fig.1.

$$l(z) = \kappa \int_{-\infty}^{z} \frac{c_{max} - c(\zeta)}{c_{max}} d\zeta, \tag{10}$$

where κ is the Karman constant(=0.4).

b) Vertical diffusion coefficients and fall velocity of sediments

Another important factor to be modeled is the vertical mass transport of the sediments in the sheet-flow layer. This is considered to be governed by the following three factors.

1) Particle collisions,
2) Turbulence of interstitial fluid,
3) Particle settling.

Among these, the former two factors have been estimated by a similar diffusion model with a mixing length.

$$K_z = (\beta d + \alpha l)^2 \left|\frac{\partial u}{\partial z}\right| + K_0, \tag{11}$$

in which the scale of mixing is assumed to be the sum of those proportional to the particle diameter, d, and to the turbulent mixing length, l. The former scale is introduced by considering that the minimum mixing scale should be governed by the sediment diameter. The values of α and β were determined as 0.35 and 1.7 respectively so that the calculated c-profiles fit the experimental results by Horikawa et al.(1982) as well as possible. K_0 is a coefficient introduced to stabilize the numerical calculation, and was set to be $5\nu_0$ by trial and error, where ν_0 is the kinematic viscosity of the intergranular fluid. The particle settling velocity, w_f, varies with the sediment concentration, c, because of the hindered effect by particle collision. This dependence of w_f on c has been proposed by several researchers to be expressed as

$$\frac{w_f}{w_{f0}} = \left(1 - \frac{c}{c_{max}}\right)^n, \tag{12}$$

where w_{f0} is the settling velocity in the still water. Although the exponent n in this equation has been reported to have several values by the experiments, the optimal value of n for complex unsteady flow conditions such as sheet-flow can not be specified. Hence, in the present study, the value of n was set simply to be one.

(4) Boundary conditions

At the left and right boundaries of the computational domain, the periodic conditions are used for u and c. At the upper boundary, on the other hand, the conditions

$$u = U_0, \quad cw_f + K_z\frac{\partial c}{\partial z} = 0, \tag{13}$$

are imposed, where U_0 is the sinusoidally oscillating velocity at the outer edge of the sheet-flow layer. Hence the horizontal pressure gradient can be given by U_0 as

$$\frac{\partial p}{\partial x} = -\rho_0\frac{\partial U_0}{\partial t}. \tag{14}$$

where ρ_0 is the density of the pure fluid.

At the lower edge of the sheet-flow layer, the following simple rest condition is imposed, because for

unsteady two-phase flows there exist no reasonable condition such as the yielding stress for static problems.

$$u=0 \qquad \text{for } c > 0.999 c_{max}, \tag{15}$$

where the coefficient of 0.999 is a factor to allow the computational error in c so that it does not yield any unrealistic influence on the rest condition.

3. Computational results and discussion

(1) Comparison of calculated values with experimental data

To confirm the validity of the present model, it has been applied to an oscillating sheet-flow problem, for which several experimental results are available for the comparison. Figure 2 is an example showing the vertical profiles of the sediment concentration c, horizontal velocity u and sediment flux q with the experimental data by Horikawa et al.(1982), and demonstrates that the present model can simulate the overall feature of these profiles and their time evolution.

Figure 3(a) shows the phase-variation of the sheet-flow depth h, representing that the present numerical model can give almost the same magnitude of variation of h within a half-cycle, as compared with the experimental results. However, the large difference in h between the acceleration and deceleration phases as seen in the experimental result cannot be reproduced by the present model. This is due to the fact that the characteristic difference of turbulent flow structure between at acceleration and deceleration phases cannot be represented by the zero-equation turbulence closure such as the mixing length model, which we have adopted for the present formulation

Figure 3(b) shows the phase-variation within a half cycle of the instantaneous sediment transport rate Φ defined as eq.(16).

$$\Phi(t) = \frac{1}{w_{f0} d} \int_{-\infty}^{\infty} q(z,t)\, dz. \tag{16}$$

There arises appreciable discrepancy between the calculated and measured values around the peak and decelerating phases. This is mainly attributable to the fact that the magnitude of the experimental velocity exhibits smaller values at the deceleration phases as shown in Fig.2.

(2) Dependence on Shields parameter

Figures 4(a) and (b) represent the dependence of the phase-variation of h and the nondimensional sand transport rate averaged over a half cycle, Φ, on the Shields parameter, ψ_m defined as eq.(17). The figures indicate that as the Shields parameter increases, the phase-variation patterns of h and Φ become skewed shapes having their peak behind the phase of $\pi/2$.

$$\psi_m = \frac{1}{2}\frac{u_{*m}^2}{sgd}, \tag{17}$$

where u_{*m} is the maximum friction velocity, s is the specific gravity of sediments in fluid and g is the gravitational acceleration.

Figure 5 shows the relation between $\bar{\Phi}$ and u_{*m}/w_f. The full line in the figure represents the experimental formula by Sawamoto & Yamashita(1987) obtained by reexamining the formula by Madsen & Grant(1976) with their own experimental data. Comparison with this experimental line indicates that the present model can estimate the mean transport rate with acceptable magnitude, though its dependence on u_{*m}/w_f is slightly weaker than that of the experimental formula.

(3) Effect of unsteadiness

The conventional ways to estimate the sediment transport rate is based on the assumption of quasisteadiness of the sediment transport process. For example, Madsen & Grant (1976) derived a formula to estimate $\bar{\Phi}$ by assuming that the instantaneous transport rate $\Phi(t)$ can be evaluated by Brown's formula(1950) for the unidirectional steady flow. In order to investigate the validity of this assumption, the effect of the unsteadiness of the sheet-flow phenomenon has been examined.

The dashed-line in Fig.3(b) indicates the instantaneous sand transport rate calculated by the Brown's formula under the assumption of such quasisteadiness. The quasisteady value of Φ is found to exhibit rapid increase and decrease pattern around its peak phase as compared with the experimental and present computational results. This fact strongly suggests that the unsteadiness has quite important role in the sheet- flow dynamics, hence it is indispensable factor for the sheet-flow modelling.

In order to investigate this point more clearly, the calculations have been executed for various values of the oscillating period T with the same Shields parameter ψ_m. Figure 6 shows the phase-variation of the sheet-flow depth h for the three periods indicated. It is found that as the period decreases the relative magnitude of h-

variation within the a half cycle also decreases, and the depth value attains its peak at more later phase. This is closely correlated with the fact that as the oscillating period becomes shorter, the sediment pick-up and successive settling process cannot catch up with the phase-variation of the flow field without any phase lag. Existence of such strong dependence of the sheet-flow evolution on the oscillating period T indicates that we should treat the sheet-flow phenomena as a nonstationary process for its modelling.

4. Conclusions

Although the present model is still rather simple and primitive in contrast with our final goal to develop the "numerical mobile bed", the present model can estimate the essential feature of sheet-flow dynamics, such as temporal evolution of sheet-flow profiles and their overall dependence on the Shields parameter. Further the difference in the period of oscillation was found to have appreciable influence on the temporal evolution of the sheet-flow thickness, indicating the importance of unsteadiness in the sheet-flow dynamics.

References

Ahilan,R.V. and Sleath,J.F.A.(1987): Sediment transport in oscillatory flow over flat bed, J. of Hydraulic Eng., Vol.113, No.3, pp.308-322.

Bagnold, R.A. (1954): Experiments on a gravity-free dispersion of large solid spheres in a Newtonian fluid under shear. Proc. R. Soc. Lond. A225, 49-63

Bakker, W.T. and van Kesteren, W. G. M.(1986): The dynamics of oscillatory sheet follow, Proc. of 20th Int. Conf. on Coastal Eng., ASCE, pp. 940-954.

Brown, C.B.(1950): Sediment Transportation, In: Rouse H., Ed., Engineering Hydraulics, John Wiley and Sons, Inc., N.Y., 1039pp.

Eilers,H. (1941): Die Viskositat von Emulsionen hochviskoser Stoffe als Funktion der Konzentrazionen, Kolloid, Z, 97, pp. 317-321.

Horikawa,K., Watanabe,A. and Katori,S. (1982): Sediment transport under sheet flow condition, Proc. of 18th Int. Conf. on Coastal Eng., ASCE, pp.1335-1352.

Kobayashi,N. and Seo, S.N.(1985): Fluid and sediment interaction over a plane bed, J. of Hydraulic Eng., ASCE,pp.903-921.

Madsen,O.S. and Grant,W.D. (1976): Sediment transport in the coastal environment, Rept. No. 209, Dept., Civil Eng., MIT.

Nadaoka,K. Ueno,S. and Yagi,H.(1988): A theoretical analysis of sheet flow under wave motion, 35th Japanese

Conf. on Coastal Eng., pp. 292-296,(in Japanese).
Nadaoka,K. Yagi,H. and Ueno,S. (1990): A weighted residual analysis of sheet-flow under wave motion, (in preparation).
Sawamoto,M. and Yamashita,T. (1987): Sediment transport in sheet flow regime, Coastal Sediments '87, ASCE,pp. 415-423.

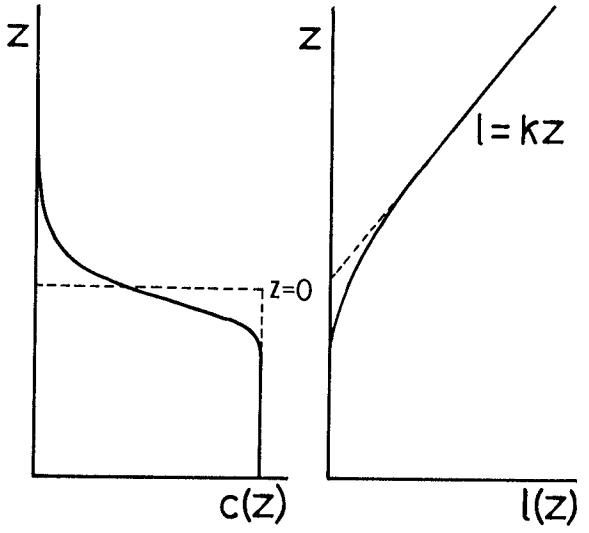

Figure 1 Conceptual illustration of the mixing length $l(z)$ corresponding to a c-profile.

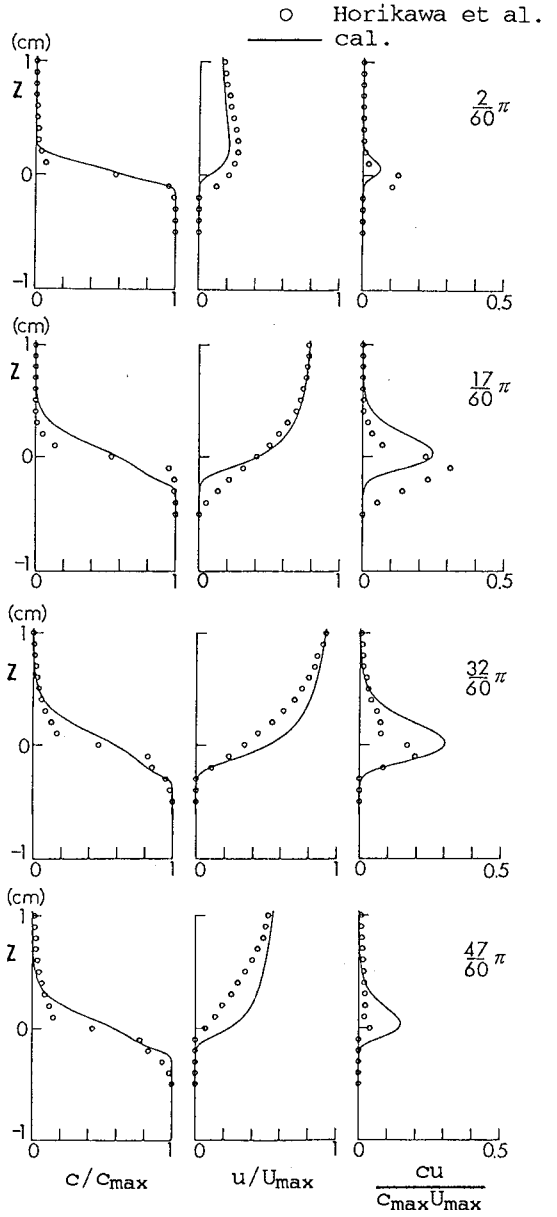

Figure 2 Vertical profiles of c, u, and q at various phases. (T = 3.6s, U_{max} = 126cm/s and d = 0.02cm.)

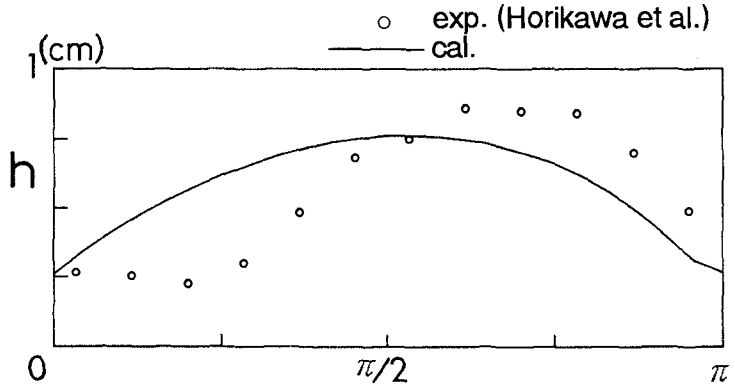

Figure 3(a) Phase-variation of the sheet-flow depth, h.

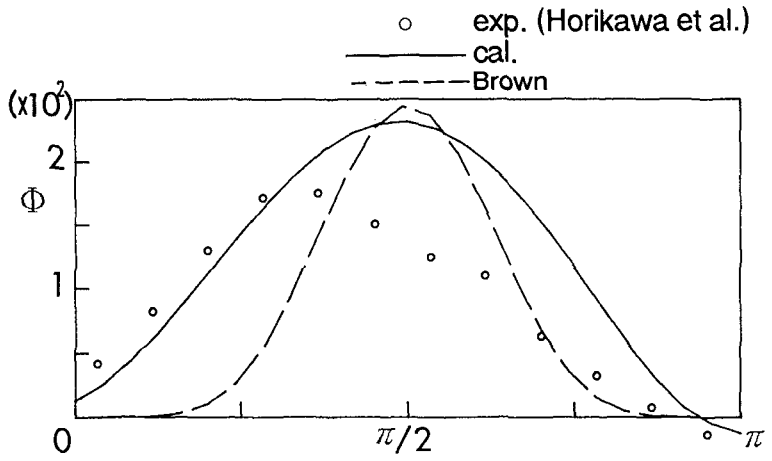

Figure 3(b) Phase-variation of the nondimensional sediment transport rate, Φ.
(T = 3.6s, U_{max} = 126cm/s and d = 0.02cm)

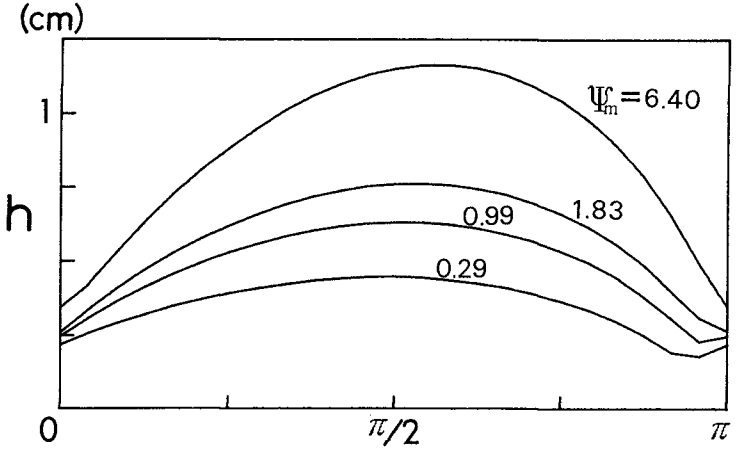

Figure 4(a) Dependence of the phase-variation of h on Ψ_m.

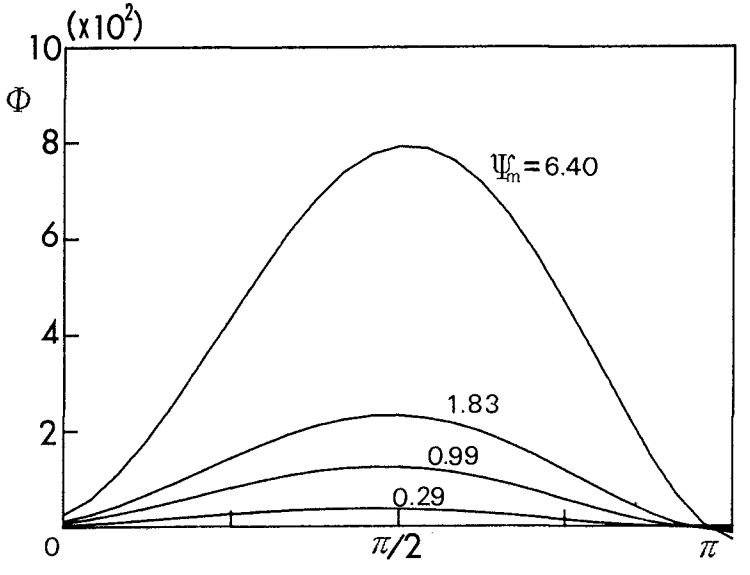

Figure 4(b) Dependence of the phase-variation of Φ on Ψ_m.

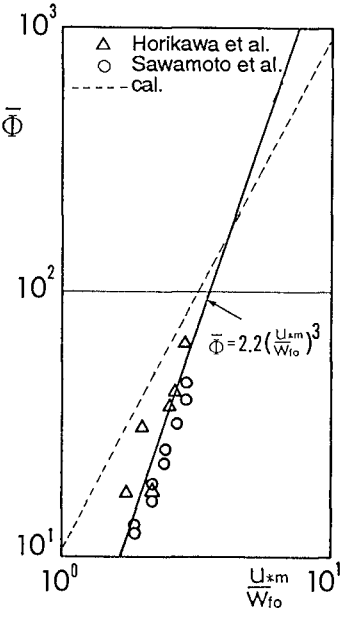

Figure 5 Relation between $\bar{\Phi}$ and u_{*m}/w_{fo}.

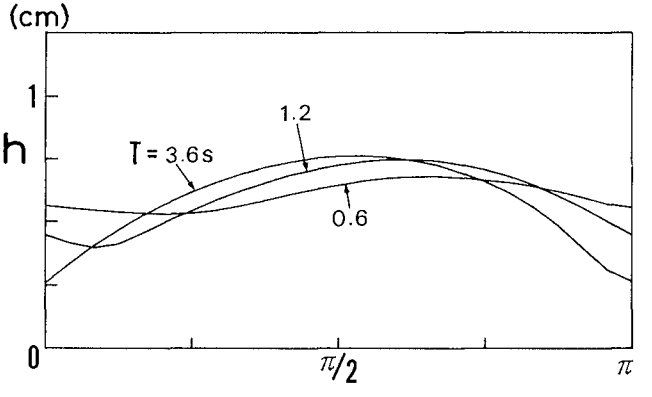

Figure 6 Dependence of the phase-variation of h on T.